Kidney360

Blood Flow Regulates Glomerular Capillary Formation in Zebrafish Pronephros

Yusuke Nishimura,[1] *Tomohiro Ishii*,[1] *Koji Ando*,[1] *Shinya Yuge*,[1] *Hiroyuki Nakajima*,[2] *Weibin Zhou*,[3] *Naoki Mochizuki*,[2] *and Shigetomo Fukuhara*[1]

Key Points

- During glomerular capillary formation, endothelial cells sprout from the dorsal aorta and surround the bilateral glomerular primordia.
- Blood flow maintains tubular structures of the capillaries surrounding the glomerular primordia.
- Blood flow also promotes glomerular incorporation of blood vessels by inducing glomerular remodeling.

Abstract

Background The renal glomerulus is a tuft of capillaries in Bowman's capsule and functions as a blood-filtration unit in the kidney. The unique glomerular capillary tuft structure is relatively conserved through vertebrate species. However, the morphogenetic mechanism governing glomerular capillary tuft formation remains elusive.

Methods To clarify how glomerular capillaries develop, we analyzed glomerular capillary formation in the zebrafish pronephros by exploiting fluorescence-based bio-imaging technology.

Results During glomerular capillary formation in the zebrafish pronephros, endothelial cells initially sprouted from the dorsal aorta and formed the capillaries surrounding the bilateral glomerular primordia in response to podocyte progenitor-derived vascular endothelial growth factor-A. After formation, blood flow immediately occurred in the glomerular primordia-associated capillaries, while in the absence of blood flow, they were transformed into sheet-like structures enveloping the glomerular primordia. Subsequently, blood flow induced formation of Bowman's space at the lateral sides of the bilateral glomerular primordia. Concomitantly, podocyte progenitors enveloped their surrounding capillaries while moving toward and coalescing at the midline. These capillaries then underwent extensive expansion and remodeling to establish a functional glomerular capillary tuft. However, stopping blood flow inhibited the remodeling of bilateral glomerular primordia, which therefore remained unvascularized but covered by the vascular sheets.

Conclusions We delineated the morphogenetic processes governing glomerular capillary tuft formation in the zebrafish pronephros and demonstrated crucial roles of blood flow in its formation. Blood flow maintains tubular structures of the capillaries surrounding the glomerular primordia and promotes glomerular incorporation of these vessels by inducing the remodeling of glomerular primordia.

KIDNEY360 3: 700–713, 2022. doi: https://doi.org/10.34067/KID.0005962021

Introduction

The kidney is a highly vascularized organ, filtering waste and toxins from the blood and then returning this blood to the body (1,2). The renal glomerulus, a tuft of capillaries, functions as a blood-filtration unit, mainly consisting of endothelial cells (ECs), podocytes, and mesangial cells. Mammalian glomerular capillary tuft formation proceeds along with glomerular morphogenesis, which occurs through several defined stages, including the renal vesicle, comma-shaped body, S-shaped body, capillary loop, and maturation stages (3,4). In the S-shaped body stage, a single capillary loop invades the glomerular cleft located between the podocyte precursors and presumptive proximal tubule (3), which depends on vascular endothelial growth factor (VEGF)-A released from podocyte precursors (5,6). Then, the initial capillary loop divides into six to eight vascular loops (7), which subsequently undergo extensive remodeling and expansion to establish a complex glomerular capillary tuft during the maturation stage. However, the morphogenetic mechanism governing establishment of glomerular capillary tufts remains unclear.

Kidney organoids have been generated from embryonic stem cells and induced pluripotent stem cells (iPSCs) *in vitro* (8–10). However, the glomeruli in

[1]Department of Molecular Pathophysiology, Institute for Advanced Medical Sciences, Nippon Medical School, Tokyo, Japan
[2]Department of Cell Biology, National Cerebral and Cardiovascular Center Research Institute, Osaka, Japan
[3]Division of Nephrology, Department of Medicine, Icahn School of Medicine at Mount Sinai, New York

Correspondence: Dr. Shigetomo Fukuhara, Department of Molecular Pathophysiology, Institute for Advanced Medical Sciences, Nippon Medical School, 1-1-5 Sendagi, Bunkyo-ku, Tokyo, 113-8602, Japan. Email: s-fukuhara@nms.ac.jp

the *in vitro* organoids remain largely avascular (9,11), although they become highly vascularized when transplanted into mice (11,12). These findings suggest that *in vivo* environments, which do not exist in a typical *in vitro* culture system, are required for glomerular vascularization.

Zebrafish have been used to study kidney development, disease, and regeneration (13–17). The zebrafish initially develops a simple embryonic kidney, known as the pronephros, which functions until the early larval stage (13–15,18). Thereafter, the mesonephros, consisting of several hundred nephrons, is established as an adult kidney (19,20). The zebrafish pronephros is composed of two nephrons that connect to a common glomerulus located ventral to the dorsal aorta (DA). The basic glomerular structures and segmental organization are relatively well conserved between the zebrafish pronephros and the mammalian metanephros (18,21). Indeed, the glomerular capillary tuft in the zebrafish pronephros possesses an architecture remarkably similar to that of the mammalian metanephros (18). Herein, we investigated glomerular capillary formation in the zebrafish pronephros and identified the precise morphogenetic processes allowing formation of a complex glomerular capillary tuft. Furthermore, we demonstrated crucial roles of blood flow in glomerular capillary tuft development.

Materials and Methods

Zebrafish Husbandry

AB strain zebrafish (*Danio rerio*) were bred, grown, and maintained on a 14-hour/10-hour light/dark cycle at 28°C, as previously described (22). Embryos and larvae used for the experiments were staged according to Kimmel *et al.* (23). Animal experiments were approved by and performed in accordance with the guidelines established by the animal committees of the Nippon Medical School.

Plasmids and Bacterial Artificial Chromosome DNAs

The Tol2 vector system was kindly provided by K. Kawakami (National Institute of Genetics, Mishima, Japan) (24). Tol2_amp and pCS2_Gal4FF_KanR vector for bacterial artificial chromosome (BAC) recombineering were kindly provided by S. Schulte-Merker (University of Münster, Münster, Germany). pCS2_deGFP_KanR was generated by replacing Gal4FF in pCS2_Gal4FF_KanR vector with a PCR-amplified destabilized enhanced green fluorescent protein (deGFP) cDNA.

BAC DNAs encoding Gal4FF and deGFP under *wt1a* and *vegfaa* promoters were constructed using the BAC clones CH73–205N6 and CH73–18P10 (BacPAC Resources, Oakland, CA), respectively, according to a method described previously (25,26). Briefly, the pRedET plasmid (Gene Bridges, Heidelberg, Germany) was transferred into the BAC clone-containing *Escherichia coli* by electroporation. Then, the DNA fragment encoding an ampicillin-resistant gene flanked by two Tol2 long terminal repeats in opposing directions was amplified by PCR using Tol2_amp vector as a template and was then inserted into the BAC vector backbone. Subsequently, the DNA fragments encoding Gal4FF and deGFP together with a kanamycin-resistant gene (Gal4_KanR and deGFP_KanR) were amplified by PCR using pCS2_Gal4FF_KanR and pCS2_deGFP_KanR vectors as templates and inserted into the start ATG codon of the *wt1a* and *vegfaa* genes, respectively. Primers used to amplify the Gal4_KanR and deGFP_KanR cDNA fragments are as follows (lowercase; homology arm to BAC vector, uppercase; primer binding site to the template plasmid): Gal4_KanR for CH73–205N6, 5′-tggaccttgtgactcaactgggccc-atttgctctgctcctgaaagtcctcaccATGAAGCTACTGTCTTCTAT-CGAAC-3′ and 5′-agcggtggaactggagggagaagagtgttgaggtc-acgaacatcagaaccTCAGAAGAACTCGTCAAGAAGGCG-3′; deGFP_KanR for CH73–18P10, 5′-taattgttttgagagccagag-actcaccgcaacactccactggaattacaaccATGGTGAGCAAGGGC-GAGGAG-3′ and 5′-agatggaggagagccgcgagaaataactgtatcaa-ataaacaaccaagttTCAGAAGAACTCGTCAAGAAGGCG-3′.

Transgenic Zebrafish Lines

To generate the *TgBAC(wt1a:gal4FF)*^{nf7Tg} and *TgBAC-(vegfaa:deGFP)*^{ncv535} zebrafish lines, the corresponding BAC DNAs (50 pg) were microinjected along with Tol2 transposase RNA (25 pg) into one-cell stage embryos of *Tg(UAS:eGFP)* and wild-type strain, respectively. Tol2 transposase mRNA was *in vitro* transcribed with SP6 RNA polymerase from *Not*I-linearized pCS-TP vector using the mMESSAGE mMACHINE kit (Ambion, Austin, TX). The embryos transiently expressing eGFP were selected, raised to adulthood, and crossed with wild-type AB to identify germline-transmitting founder fishes.

Tg(wt1a:eGFP), *Tg(kdrl:tagBFP)*^{mu293Tg}, and *Tg(UAS:eGFP)* zebrafish lines were kindly provided by Christoph Englert (Leibniz Institute on Aging–Fritz Lipmann Institute, Jena, Germany), D.Y. Stainier (Max Planck Institute for Heart and Lung Research, Bad Nauheim, Germany) (27), and K. Kawakami (National Institute of Genetics, Mishima, Japan) (28), respectively. *Tg(fli1a:Myr-mCherry)*^{ncv1Tg} (22), *Tg(wt1a:eGFP)* (27), *Tg(podocin:NTR-mCherry)* (29), *Tg(UAS:-NTR-mCherry)* (29), *Tg(pdgfrb:eGFP)*^{ncv22Tg} (26), and *Tg-(UAS:loxP-mCherry-loxP-mVenus)*^{ncv28Tg} (26) zebrafish lines were previously described.

Image Acquisition and Processing

To acquire images of the zebrafish pronephros, the pigmentation of embryos and larvae was inhibited by treatment with 1-phenyl-2-thiourea (PTU; Sigma–Aldrich, St. Louis, MO). The embryos and larvae at 28–120 hours post fertilization (hpf) were anesthetized with E3 embryo medium containing 0.016% tricaine (Sigma–Aldrich) and fixed in 4% paraformaldehyde in PBS (Nacalai Tesque, Kyoto, Japan) for 30 minutes or 1 hour at room temperature. After washing with PBS, the yolk sac was carefully removed with a 27-gauge needle (Terumo) to expose the pronephros. Then, the yolk sac–removed embryos or larvae were mounted ventral side up in 1% low-melting agarose dissolved in E3 medium poured onto a 35-mm glass-based dish (Iwaki, Asahi Glass Co. Ltd., Tokyo, Japan) as shown in Figure 1A, and then immersed in PBS. Confocal images were obtained with a FluoView FV1200 or FV3000 confocal upright microscope system (Olympus, Tokyo, Japan) with a ×20 water immersion lens (XLUMPlanFL, NA=1.0) and a multi-alkali or a GaAsP photomultiplier tube operated with FLUOVIEW FV10ASW or FluoView FV31S SW software (Olympus). Lasers with excitation wavelengths of

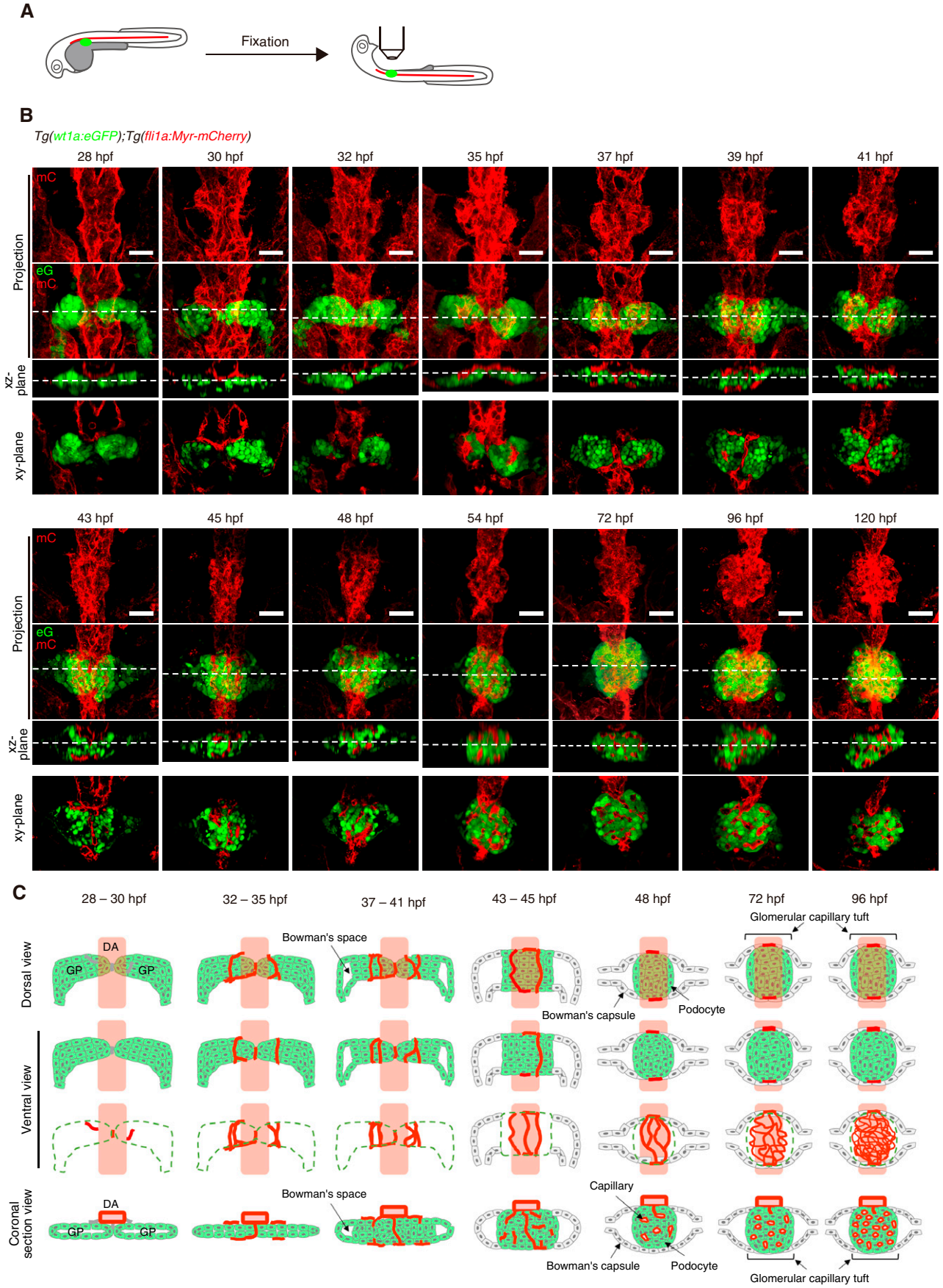

Figure 1. | **Morphogenetic processes of glomerular capillary formation in zebrafish pronephros.** (A) Schematic illustration showing a sample preparation procedure and imaging of the zebrafish pronephros. After removal of the yolk sac from the fixed embryos and larvae,

405, 488, and 546 nm were used. Fluorescence images were acquired sequentially to avoid cross-detection of the fluorescent signals. The confocal images obtained were processed using Volocity 3D Imaging Analysis software (Quorum Technologies, Laughton, United Kingdom).

Live Imaging of Zebrafish Pronephros

To analyze blood circulation in the glomerular capillaries, *Tg(wt1a:eGFP);Tg(fli1a:Myr-mCherry)* embryos were dechorionated, anesthetized in 0.016% tricaine in E3 medium, and embedded lateral side up in 1% low-melting agarose dissolved in E3 medium poured onto a 35-mm glass-based dish. Then, approximately 0.5–1 nl of Qtracker 705 Vascular Labels (Thermo Fisher Scientific, Waltham, MA) was injected into the common cardinal vein of the embryos using an IM-300 microinjector (Narishige). After confirming circulation of the intravascular-injected Qtracker 705 using a SZX16 stereomicroscope (Olympus), the embryos were extracted and remounted dorsal side up in 1% low-melting agarose as shown in Figure 3A. Confocal images were obtained with a FluoView FV3000 confocal upright microscope system with a ×20 water immersion lens (XLUMPlanFL, NA=1.0) and a GaAsP photomultiplier tube operated with FluoView FV31S SW software as described above. Image files were processed and analyzed using the Volocity 3D Imaging Analysis software and the Fiji (http://fiji.sc.) image processing package.

To analyze zebrafish pronephros morphogenesis, *Tg(wt1a:eGFP);Tg(fli1a:Myr-mCherry)* embryos were mounted dorsal side up in 1% low-melting agarose dissolved in E3 medium poured onto a 35-mm glass-based dish. The mounted embryos were submerged in E3 medium supplemented with 0.016% tricaine and 0.2 mM PTU. For confocal time-lapse imaging, eGFP and Myr-mCherry fluorescence images were acquired every 15 minutes for approximately 15 hours using a FluoView FV3000 confocal upright microscope system as described above. During the time-lapse imaging, room temperature was set to 28°C. The z-stack images obtained were then 3D volume rendered with fluorescence mode using Volocity 3D Imaging analysis software.

Drug Treatment

The following drugs were used to treat the zebrafish embryos and larvae: 20 mM 2,3-butanedione monoxime (BDM; Sigma–Aldrich), 1 μM Ki8751 (ChemScene, Monmouth Junction, NJ), and SC-3BT (Abcam, Cambridge, United Kingdom). The drugs were dissolved in E3 medium supplemented with PTU. DMSO (Nacalai Tesque) was dissolved in the E3 medium as the control for the Ki8751 treatment.

Results

Morphogenetic Processes of Glomerular Capillary Tuft Formation in Zebrafish Pronephros

We imaged the processes of glomerular capillary formation in *Tg(wt1a:eGFP);Tg(fli1a:Myr-mCherry)* zebrafish (Figure1A). At 28 hpf, bilateral *wt1a:eGFP*-positive unvascularized glomerular primordia were located ventral to the DA (Figure 1, Supplemental Movie 1). A few hours later, Myr-mCherry-labeled ECs sprouted from the lateral sides of the DA and extended toward the glomerular primordia. Vessels also sprouted from the ventral side of the DA and invaded the area between the bilateral glomerular primordia. At 32–35 hpf, the vessel sprouts from the DA further elongated, surrounded the glomerular primordia while aligning in parallel along the DA, and connected to the ventrally invading vessels (Figure 1, Supplemental Movie 2). At 37–41 hpf, the bilateral glomerular primordia coalesced at the midline to enclose the ventrally invading vessels (Figure 1, Supplemental Movie 3). Simultaneously, the podocyte progenitors in the glomerular primordia moved slightly toward the midline, leading to the formation of Bowman's space at the lateral sides. Medial movement of the podocyte progenitors resulted in the vessels surrounding the glomerular primordia being partially buried in them. At 43–45 hpf, Bowman's space showed further expansion. Concomitantly, the podocyte progenitors further medially moved to enclose the blood vessels, leading to formation of a single glomerulus containing several blood vessels aligned in parallel to the DA. These vessels had partially connected to each other, establishing a primitive capillary network, at 48 hpf (Figure 1, Supplemental Movie 4). Thereafter, extensive remodeling generated a more complex glomerular capillary tuft (Figure 1, Supplemental Movie 5). These observations indicate that during glomerular capillary formation in the zebrafish pronephros, ECs initially sprout from the DA and form the capillaries surrounding the glomerular primordia through sprouting angiogenesis. These vessels are subsequently incorporated into the glomerular primordia and undergo extensive expansion and remodeling, establishing a glomerular capillary tuft (Figure 1C).

Figure 1. (*Continued*) they were mounted ventral side up in 1% low-melting agarose and imaged as described in the Materials and Methods section. (B) Confocal z-projection and single-plane images of the zebrafish pronephros in *Tg (wt1a:eGFP);Tg(fli1a:Myr-mCherry)* embryos and larvae at the stage indicated at the top of each column. Ventral views; anterior to the top. The first and second rows show z-projection images of *fli1a:Myr-mCherry* (mC; red) and the merged images of *wt1a:eGFP* (eG; green) and *fli1a:Myr-mCherry* (mC; red), respectively. The third row is cross-sectional single-plane images (xz-plane) of the areas indicated by dotted lines on the images in the second row. The bottom row shows the xy-single slice images of the areas indicated by dotted lines on the xz-plane images. Scar bars: 20 μm. (C) Schematic drawings of the glomerular structures in the zebrafish pronephros at the stage indicated at the top of each column. Green indicates *wt1a:eGFP*-positive glomerular primordia and podocytes, whereas red shows *fli1a:Myr-mCherry*-positive blood vessels. The first row is the dorsal view images of the glomeruli, whereas the second and third rows are the ventral view images that correspond to the z-projection images in (B). In the third row, the *wt1a:eGFP*-positive glomerular primordia and podocytes are indicated by dotted green lines. The bottom row shows the coronal section views of the glomeruli corresponding to the cross-sectional single-plane images in (B). GP, glomerular primordia; DA, dorsal aorta.

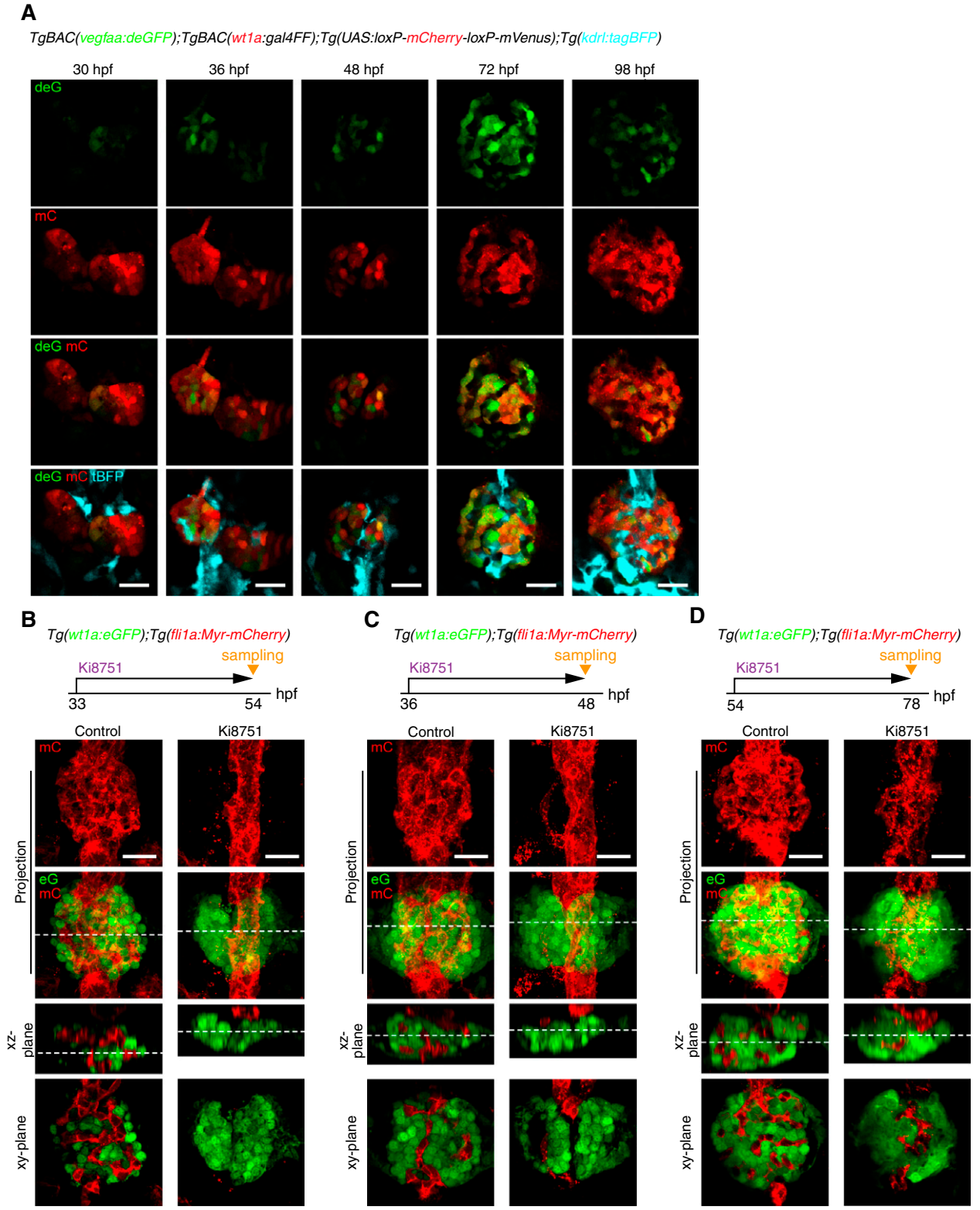

Figure 2. | **Requirement of Vegf signaling for glomerular capillary formation.** (A) Confocal single z-plane images of pronephric glomeruli in *TgBAC(vegfaa:deGFP);TgBAC(wt1a:gal4FF);Tg(UAS:loxP-mCherry-loxP-mVenus);Tg(kdrl:tagBFP)* embryos and larvae at the stage indicated at the top of each column. Ventral view images of the fixed embryos and larvae were acquired as shown in Figure 1A. Ventral views; anterior to the top. First row, *vegfaa:deGFP* fluorescence (deG; green); second row, *wt1a:gal4FF;UAS:loxP-mCherry-loxP-mVenus* fluorescence (mC, red); third row, the merged images of deG and mC fluorescence; fourth row, the merged images of deG, mC, and *kdrl:tagBFP* (tBFP, cyan). Scale bars; 20 μm. (B–D) Effects of Ki8751, a Vegf receptor inhibitor, on glomerular capillary formation. Confocal fluorescence images of the pronephric glomeruli in *Tg(wt1a:eGFP);Tg(fli1a:Myr-mCherry)* zebrafish treated with DMSO (control) or with 1 μM Ki8751 from 33 to 54 hpf (B), from 36 to 48 hpf (C), and from 54 to 78 hpf (D). The z-projection and single-plane images are shown as Figure 1B. Scale bars; 20 μm. Vegf, vascular endothelial growth factor; deGFP, destabilized enhanced green fluorescent protein; hpf, hours post fertilization.

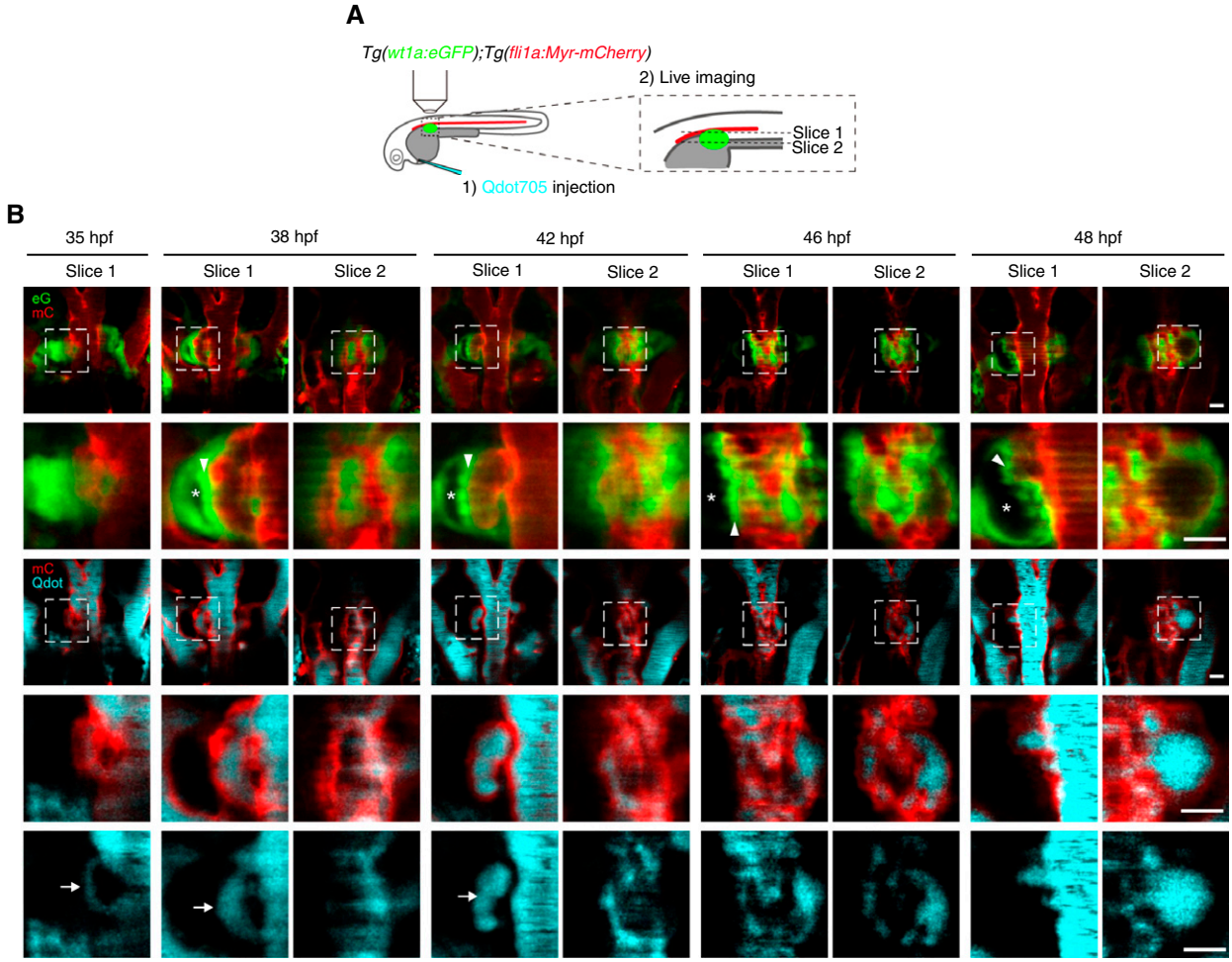

Figure 3. | **Blood circulation in the capillaries during glomerular morphogenesis.** (A) Schematic illustration showing the experimental procedure to visualize the blood flow in glomerular capillaries. *Tg(wt1a:eGFP);Tg(fli1a:Myr-mCherry)* embryos were intravascularly injected with Qdot705, mounted dorsal-side up in 1% low-melting agarose, and imaged with a confocal upright microscope as described in the Materials and Methods section. (B) Single z-plane images showing the dorsal (slice 1) and ventral (slice 2) parts of the glomerular primordia or glomeruli in *Tg(wt1a:eGFP);Tg(fli1a:Myr-mCherry)* embryos injected intravascularly with Qdot705 at the stages indicated at the top. Dorsal views; anterior to the top. The first and third rows show the merged images of *wt1a:eGFP* (eG; green) and *fli1a:Myr-mCherry* (mC; red) and those of *fli1a:Myr-mCherry* (mC; red) and Qdot705 (Qdot, cyan), respectively. The boxed areas on the images in the first and third rows are enlarged in the second and fourth rows, respectively. Qdot705 images in the boxed areas in the third row are enlarged in the bottom row. Arrows, Qdot705 circulating in the vessels surrounding the glomerular primordia; arrowheads, podocytes, or podocyte progenitors moving toward the midline; asterisks, Bowman's space. Scale bars: 20 μm.

Differentiation of Podocytes and Mesangial Cells in Zebrafish Pronephros

Next, we analyzed podocyte differentiation during glomerular development by imaging *Tg(podocin:NTR-mCherry)* zebrafish expressing NTR-mCherry in mature podocytes (Supplemental Figure 1) (29). The *podocin:NTR-mCherry* signal was initially detected in the *wt1a:eGFP*-positive cells located at the midline at 48 hpf. Thereafter, most of the *wt1a:eGFP*-positive cells became positive for the *podocin:NTR-mCherry* signal, suggesting that podocyte progenitors terminally differentiate upon reaching the midline.

We also investigated mesangial cell differentiation by imaging *TgBAC(pdgfrb:eGFP)* zebrafish expressing eGFP in mural cells (Supplemental Figure 2) (26). The *pdgfrb:eGFP*-positive cells appeared in perivascular regions within the glomerular primordia at 36 hpf, and their emergence continued along with the growth of glomerular capillaries. These results suggest glomerular capillaries play a role in mesangial cell differentiation. Furthermore, *wt1a:GAL4*-driven expression of NTR-mCherry was rarely detected in the *pdgfrb:eGFP*-positive cells, suggesting that the origin of mesangial cells differs from that of podocytes.

Formation and Maintenance of Glomerular Capillaries by Podocyte-Derived Vegfa

During glomerular morphogenesis, VEGF-A released from the presumptive podocytes regulates glomerular capillary formation in mice (5,6). Therefore, we investigated whether Vegfa regulates glomerular capillary formation in the zebrafish pronephros. To analyze *vegfa* expression in the developing glomerulus, we generated *TgBAC(vegfaa:deGFP)* zebrafish in which deGFP was expressed under the control of the *vegfaa* promoter. The *TgBAC(vegfaa:deGFP)*

embryos at 28 hpf exhibited deGFP fluorescence in those somites in which *vegfa* is known to be expressed (30), indicating that this reporter line precisely recapitulates endogenous *vegfa* expression (Supplemental Figure 3). Consistent with a previous report showing *vegfa* mRNA expression in differentiating podocytes (31), the *vegfaa:deGFP* signal was detected in *wt1a*-positive glomerular primordia at least from 30 hpf (Figure 2A). Thereafter, this signal increased and was confined to the podocytes within a glomerulus at later stages, suggesting that both differentiating and mature podocytes express *vegfa*.

Furthermore, we investigated the role of Vegf signaling for glomerular capillary formation utilizing an inhibitor of VEGF receptors, Ki8751 (32). Ki8751 treatment from 33 hpf completely suppressed vessel sprouting from the DA, leading to the formation of unvascularized glomeruli at 54 hpf (Figure 2B), indicating that Vegf signaling induces EC sprouting from the DA. Ki8751 treatment from 36 to 48 hpf resulted in partial regression of the blood vessels associated with glomerular primordia (Figure 2C). Similarly, the glomerular capillaries showed partial regression in response to Ki8751 treatment from 54 to 78 hpf (Figure 2D). These findings indicate that Vegf signaling maintains the glomerular capillaries throughout glomerular development. Taken together, these results suggest Vegfa, probably produced by differentiating and mature podocytes, regulates the formation and maintenance of glomerular capillary tufts.

Timing of Blood Circulation Onset in Glomerular Capillaries

We next determined the timing of blood circulation onset in glomerular capillaries by intravascularly injecting Qdot705 (Figure 3) because DA-derived ECs initially formed the vessels surrounding the glomerular primordia before entering the glomerulus. When Qdot705 was injected into the circulatory system at 35 hpf, a weak Qdot705 signal was detected in the vessels surrounding glomerular primordia, indicating that blood circulation starts immediately after their formation (Figure 3B, Supplemental Movie 6). At 38 hpf, the vessels associated with the glomerular primordia became enlarged and exhibited clear Qdot705 signals (Figure 3B, Supplemental Movie 7). Simultaneously, Bowman's space appeared on the lateral sides of the glomerulus along with medial displacement of podocyte progenitors. At 42 hpf, several blood vessels aligned along the DA were incorporated into the glomerulus and showed circulation of intravascularly injected Qdot705 (Figure 3B, Supplemental Movie 8). Subsequently, circulation of Qdot705-containing blood was detected in the primitive capillary networks within the glomerulus at 46–48 hpf (Figure 3B, Supplemental Movies 9 and 10). These results indicate that blood circulation begins when the blood vessels sprouting from the DA surround the glomerular primordia and continues during glomerular incorporation of these vessels. We also observed medial displacement of podocyte progenitors and formation of Bowman's space to occur simultaneously along with blood circulation onset in developing glomerular capillaries, suggesting that blood flow might trigger the remodeling of glomerular primordia.

Blood Flow Requirement for Glomerular Capillary Formation

We further investigated the role of blood flow in glomerular capillary morphogenesis by arresting the heartbeat. We treated *Tg(wt1a:eGFP);Tg(fli1a:Myr-mCherry)* embryos from 25 hpf with BDM, an inhibitor of skeletal muscle myosin-II (33) (Figure 4A). At 32–34 hpf, the vessels sprouting from the DA extended toward the bilateral glomerular primordia in control and BDM-treated embryos, indicating that blood flow is dispensable for EC sprouting from the DA (Figure 4B). In control embryos, the vessels subsequently surrounded the glomerular primordia at 37 hpf, whereas the DA-derived ECs formed sheet-like structures enveloping the glomerular primordia in BDM-treated embryos (Figure 4B). At 39 hpf, blood vessels aligned along the DA were partially incorporated into the glomerular primordia that coalesced at the midline in controls (Figure 4B). However, the vascular sheets formed by the DA-derived ECs entirely covered the bilateral glomerular primordia, which failed to assemble in BDM-treated embryos (Figure 4B). These results suggest that blood flow maintains tubular structures of blood vessels associated with glomerular primordia.

Next, to explore the role of blood flow in glomerular incorporation of blood vessels, we arrested the heartbeat in the 36 hpf embryos that exhibit glomerular primordia surrounded by DA-derived vessels. We treated the embryos with either BDM or tricaine, an anesthetic agent inhibiting heartbeat through a mechanism distinct from that of BDM (34,35) (Figure 4C). At 54 hpf, the glomeruli in control embryos were highly vascularized by glomerular capillaries (Figure 4, D and E, Supplemental Movie 11). However, treatment with either BDM or tricaine inhibited assembly of glomerular primordia and their inclusion of blood vessels (Figure 4, D and E, Supplemental Movies 12 and 13). Instead, the DA-derived ECs formed vascular sheets to cover the bilateral glomerular primordia entirely. This finding is consistent with a previous report showing zebrafish mutants lacking circulation to display bilateral glomerular primordia surrounded by DA-derived ECs (36). These findings suggest that blood flow maintains the tubular structures of blood vessels surrounding glomerular primordia and also regulates glomerular assembly and vascular invasion into the glomerulus.

Role of Matrix Metalloproteinases in Glomerular Capillary Formation

Blood flow–induced expression of matrix metalloproteinase (MMP) 2 in ECs reportedly regulates assembly of bilateral glomerular primordia (36). Thus, we investigated whether blood flow regulates glomerular capillary formation through expression of endothelial MMP2. For this purpose, we examined the effects of SB-3CT, an inhibitor of MMP2 and MMP9 (37), on glomerular capillary formation (Figure 4F). SB-3CT treatment from either 25 or 33 hpf to 54 hpf resulted in defective glomerular assembly, confirming SB-3CT effectiveness (Figure 4G). In addition, ECs did not sprout from the DA in the embryos treated with SB-3CT from 25 hpf, suggesting that ECs might sprout from the DA by producing MMPs to degrade the extracellular matrix (Figure 4G). However, SB-3CT treatment from 33 hpf did not inhibit vascular invasion into the bilateral

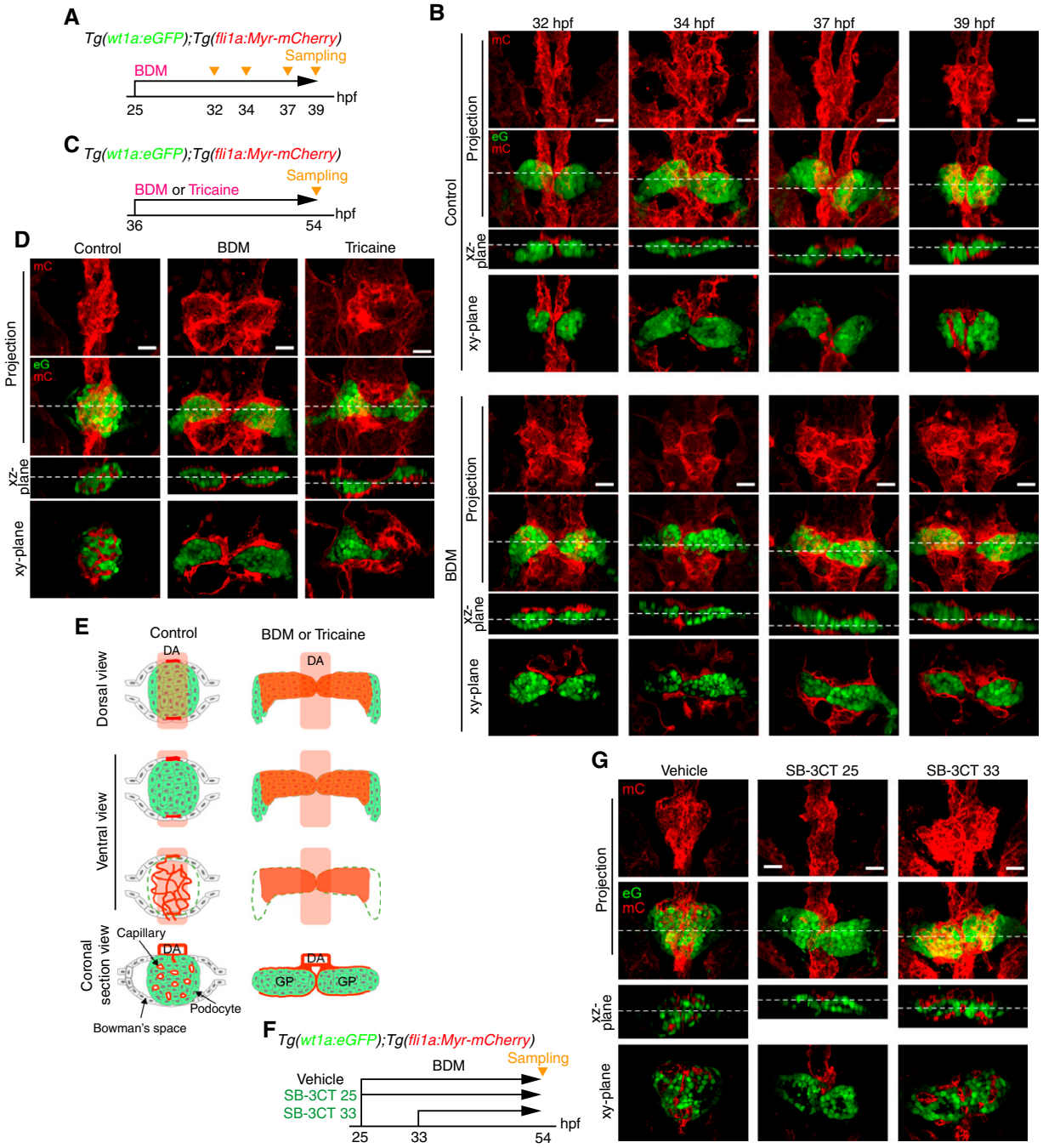

Figure 4. | **Requirement of blood flow for glomerular capillary formation.** (A–E) Effects of stopping blood flow on glomerular capillary formation. (A and B) *Tg(wt1a:eGFP);Tg(fli1a:Myr-mCherry)* embryos were treated with vehicle (upper panel in B) or BDM (lower panel in B) from 25 hpf and fixed with paraformaldehyde at 32, 34, 37, and 39 hpf. Subsequently, the fixed embryos were imaged with a confocal upright microscope as shown in Figure 1A. (B) The z-projection and single-plane images of the pronephric glomeruli at the stages indicated at the top are shown as in Figure 1B. Scale bars: 20 μm. (C and D) *Tg(wt1a:eGFP);Tg(fli1a:Myr-mCherry)* embryos were treated with vehicle (control), BDM, or tricaine from 36 hpf, fixed at 54 hpf, and imaged with a confocal upright microscope as shown in Figure 1A. (D) The z-projection and single-plane images of the pronephric glomeruli are shown as in Figure 1B. Scale bars: 20 μm. (E) Schematic illustration of the pronephric glomeruli in embryos treated with vehicle (control) or with BDM or tricaine as observed in (D)are shown as in Figure 1C. (F and G) Effects of SB-3CT, an inhibitor for MMP2 and MMP9, on glomerular capillary formation. *Tg(wt1a:eGFP);Tg(fli1a:-Myr-mCherry)* embryos were treated with vehicle from 25 hpf (control) or with SB-3CT from 25 (SB-3CT 25) or 33 hpf (SB-3CT 33), fixed at 54 hpf, and imaged with a confocal upright microscope as shown in Figure 1A. The z-projection and single-plane images of the pronephric glomeruli are shown as in Figure 1B. Scale bars: 20 μm. BDM, 2,3-butanedione monoxime.

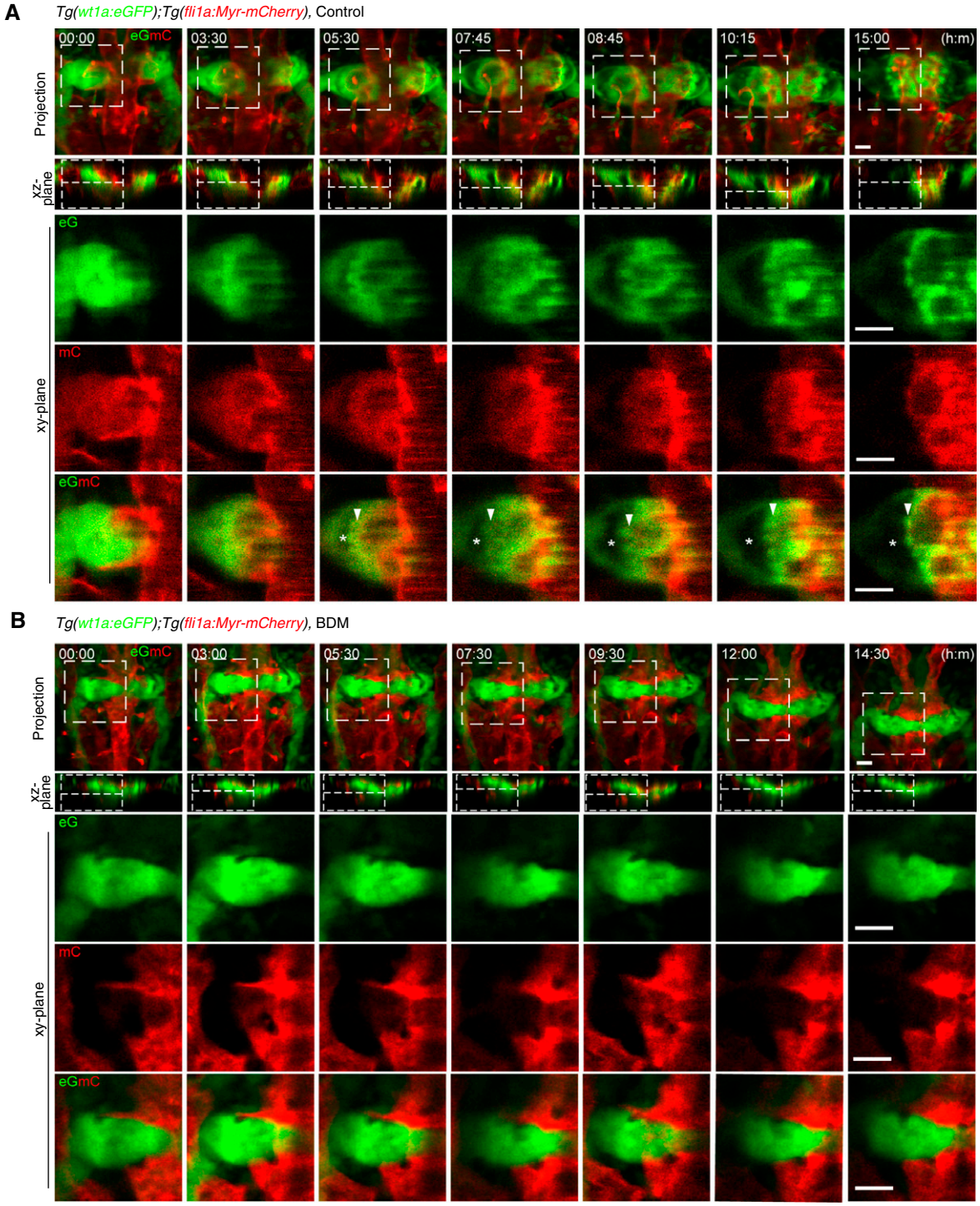

Figure 5. | **Glomerular morphogenesis in the presence and absence of blood flow.** Confocal fluorescence images of pronephric glomeruli in 33 hpf *Tg(wt1a:eGFP);Tg(fli1a:Myr-mCherry)* embryos in the absence (A) or presence (B) of BDM and the corresponding subsequent time-lapse images, obtained at the indicated time points (h:min). Merged images of z-projections of *wt1a:eGFP* (eG; green) and *fli1a:Myr-mCherry* (mC; red) are shown in the top row. The second row shows the cross-sectional single-plane images (xz-plane) of the areas indicated by dotted lines on the images in the top row. The boxed areas on the images in the first row are enlarged as xy-plane images obtained at the z-levels indicated by the dotted lines on the xz-plane images in the three rows from the bottom, in which *wt1a:eGFP* images, *fli1a:Myr-mCherry* images, and their merged images are shown in the third, fourth, and fifth rows, respectively. Arrowheads, podocytes or podocyte progenitors moving toward the midline; asterisks, Bowman's space. Scale bars: 20 μm.

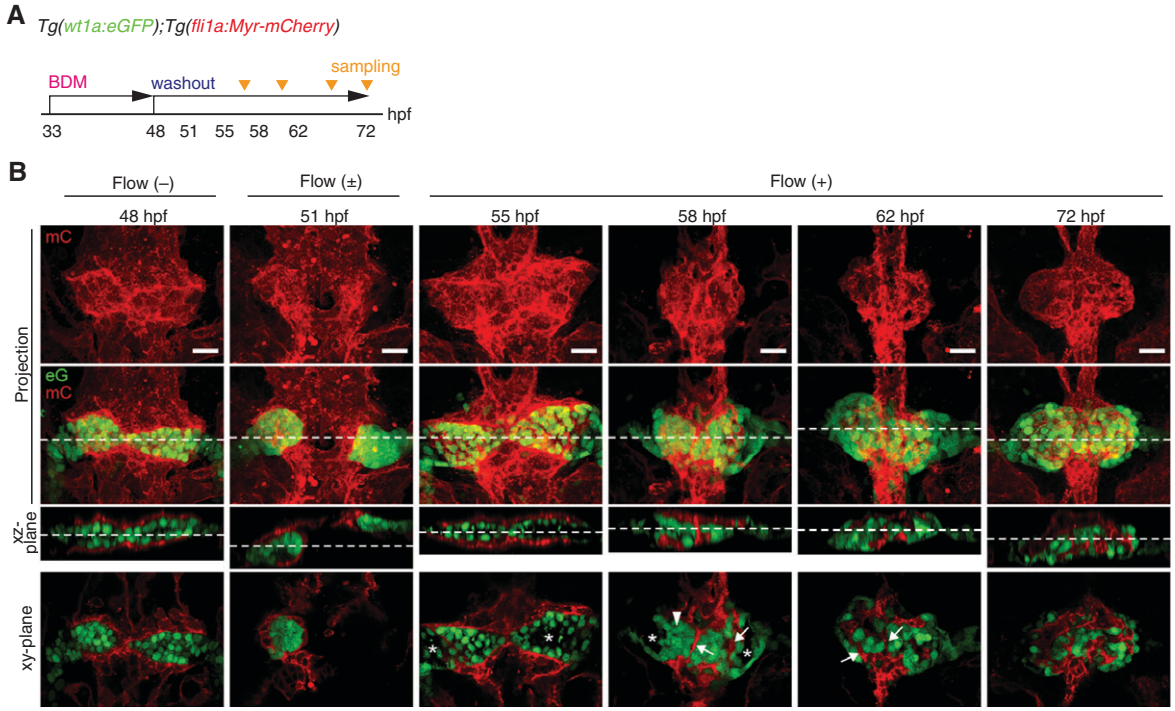

Figure 6. | Potential roles of blood filtration in glomerular remodeling and capillary formation. (A) Schematic diagram showing the experimental protocol for investigating the effects of stopping and subsequently restarting blood flow on glomerular morphogenesis and capillary formation. (B) The z-projection and single-plane images of the glomerular primordia and glomeruli in *Tg(wt1a:eGFP);Tg(fli1a:-Myr-mCherry)* embryos are shown as in Figure 1B. The 48 hpf embryos treated with BDM from 33 hpf exhibited *wt1a:eGFP*-positive bilateral glomerular primordia covered by the *fli1a:Myr-mCherry*-labeled endothelial cells sprouted from the dorsal aorta (leftmost column). After termination of BDM treatment from 48 hpf, blood circulation was detected in the embryos at 51 hpf (second column from the left). Subsequently, structural changes in the vascular sheets and the enveloping glomerular primordia associated with the onset of blood flow were analyzed at 55, 58, 62, and 72 hpf (four columns from the right). Arrowheads, blood vessels that were derived from the vascular sheets enveloping the glomerular primordia; asterisks, inner cavity formed inside the glomerular primordia or Bowman's space. Scale bars: 20 μm.

glomerular primordia (Figure 4G). These findings indicate that blood flow–induced expression of MMP2 is dispensable for glomerular incorporation of blood vessels, although vessel sprouting from the DA requires MMPs.

Blood Flow–Mediated Glomerular Inclusion of Blood Vessels through Remodeling of Glomerular Primordia

Our data showed that the timing of blood flow–dependent glomerular remodeling coincides with glomerular incorporation of blood vessels. Therefore, we tested whether blood flow–induced glomerular remodeling induces glomerular incorporation of blood vessels by time-lapse imaging the glomerular formation process from 33 hpf (Figure 5A, Supplemental Movie 14). Blood vessels sprouting from the DA surrounded the bilateral glomerular primordia at 33 hpf and became lumenized a few hours later, showing the onset of blood circulation. At the 3- to 5-hour time points, Bowman's space appeared at the lateral sides of glomerular primordia, which was accompanied by the medial displacement of podocyte progenitors. At the 7- to 10-hour time points, Bowman's space was greatly expanded by further medial movement of the podocyte progenitors. At this time, the podocyte progenitors enveloped the blood vessels associated with glomerular primordia while moving to the midline. The primitive capillary network was then established within the glomerulus at the 15-hour time point. Furthermore, we analyzed the effect of stopping blood flow on glomerular remodeling and vascular morphogenesis (Figure 5B, Supplemental Movie 15). In the absence of blood flow, the DA-derived ECs formed sheet-like structures and covered the bilateral glomerular primordia. The emergence of Bowman's space and the medial movement of podocyte progenitors did not occur in BDM-treated embryos. As a result, the bilateral glomerular primordia failing to undergo midline fusion became covered by the vascular sheets arising from DA-derived ECs and remained unvascularized even at the 14.5-hour time point. These findings suggest that blood flow in vessels surrounding the glomerular primordia induces glomerular remodeling, which results in glomerular incorporation of these blood vessels.

To confirm the importance of blood flow in glomerular capillary formation, we stopped and subsequently restarted blood flow and then analyzed glomerular morphogenesis and capillary formation (Figure 6). In the 48 hpf embryos treated with BDM from 33 hpf, the bilateral glomerular primordia were covered with the vascular sheets formed by DA-derived ECs. Then, we removed BDM from the fish water to allow heartbeat recovery and eventually detected blood circulation onset at around 51 hpf. We next analyzed

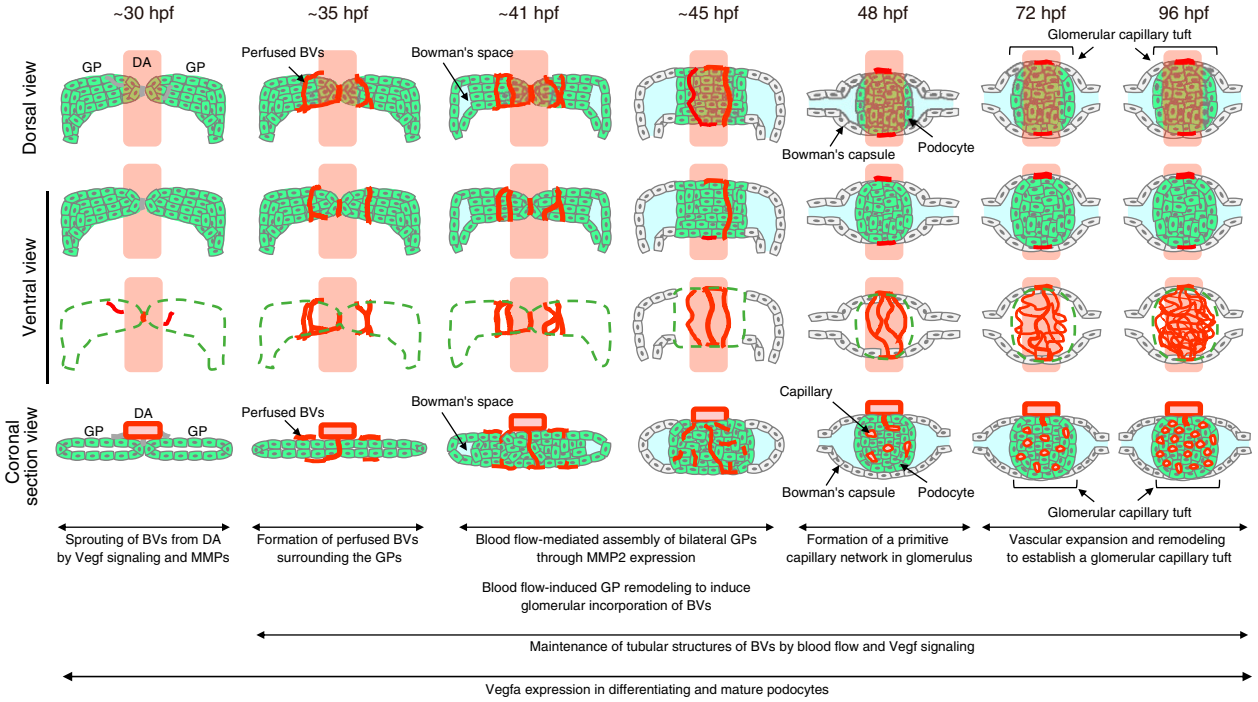

Figure 7. | **Proposed model of morphogenetic processes of glomerular capillary formation in zebrafish pronephros.** Schematic drawings of the glomerular structures in the zebrafish pronephros at the stage indicated at the top of each column. The first and second/third rows are the dorsal and ventral view images of the glomerular primordia or glomeruli, respectively. The bottom row shows the coronal section views of the glomerular primordia or glomeruli. Green, glomerular primordia or podocytes; red, blood vessels; cyan, Bowman's space. BVs, blood vessels.

structural changes in the vascular sheets and glomerular primordia associated with blood-flow onset. At 55 hpf, normal blood flow had been established, and inner cavities appeared in the bilateral glomerular primordia surrounded by vascular sheets. These vascular sheets had transformed into tubular structures at 58 hpf. Concomitantly, the podocyte progenitors moved to the midline, thereby promoting glomerular coalescence and the emergence of Bowman's space. At 62 hpf, the podocyte progenitors enveloped the vessels while coalescing at the midline. A glomerulus containing the capillary tuft as observed in the controls at 48 hpf was thereby established at 72 hpf. These results suggest that blood flow maintains the tubular structures of vessels surrounding the glomerular primordia and also promotes glomerular incorporation of these vessels by inducting glomerular remodeling.

Discussion

Herein, we delineated morphogenetic processes governing development of the glomerular capillary tuft in the zebrafish pronephros (Figure 7). At 32–35 hpf, ECs sprout from the DA and form blood vessels surrounding the bilateral glomerular primordia through sprouting angiogenesis mediated by Vegf signaling and MMPs. Subsequently, the bilateral glomerular primordia fuse at the midline and undergo remodeling, during which the blood vessels are incorporated into the glomerulus at approximately 45 hpf. Thereafter, these vessels undergo extensive remodeling to establish the glomerular capillary tuft. Importantly, we demonstrate crucial roles of blood flow in glomerular capillary formation. Blood flow maintains tubular structures of the capillaries surrounding the glomerular primordia cooperatively with Vegf signaling. Subsequently, blood flow also promotes glomerular inclusion of those vessels by inducing MMP2-independent glomerular remodeling.

During glomerular capillary formation, blood flow maintains the integrity of the capillaries surrounding the glomerular primordia. Blood flow–driven mechanical forces, with EC exposure, reportedly maintain vascular integrity (38–43). Consistently, we found that stopping blood flow resulted in vascular lumen collapse in vessels surrounding the glomerular primordia. However, these collapsed vessels showed no regression, instead being transformed into sheet-like structures to cover the glomerular primordia. Because the glomerular primordia expressed Vegfa and inhibition of Vegf signaling caused regression of the vessels associated with glomerular primordia, blood flow might work cooperatively with Vegfa to maintain the integrity of vessels surrounding these primordia.

Blood flow regulates glomerular capillary morphogenesis by inducing remodeling of glomerular primordia. Serluca *et al.* reported that zebrafish mutants showing cardiac dysfunction exhibit defective assembly of bilateral glomerular primordia and that DA-derived ECs surround them (36). Mechanistically, they demonstrated that blood flow induces MMP2 expression in ECs, which in turn promotes glomerular assembly. Consistently, this study confirmed the role of MMP2 in glomerular assembly. However, our data showed that MMP2 is not required for glomerular

incorporation of blood vessels because MMP2/9 inhibitor did not prevent vessel invasion into the glomeruli, despite inhibiting glomerular assembly. Instead, we found that blood flow induces glomerular remodeling, which involves the formation of Bowman's space and medial movement of podocyte progenitors, during which podocyte progenitors enclose the blood vessels to form the vascularized glomerulus. Thus, blood flow regulates both MMP2-dependent glomerular assembly and MMP2-independent glomerular incorporation of blood vessels to establish functional glomeruli.

How does blood flow induce glomerular remodeling to promote their inclusion of blood vessels? When blood flow began in the vessels associated with glomerular primordia, Bowman's space emerged, and the podocyte progenitors moved to and coalesced at the midline to enclose the blood vessels. These morphologic changes were abolished by stopping blood flow. Thus, blood filtration in the vessels surrounding the glomerular primordia might trigger glomerular remodeling. Consistently, blood filtration in the glomerulus reportedly begins between 36 and 48 hpf (18). Therefore, blood flow–dependent glomerular filtration might induce formation and expansion of Bowman's space, leading to movement of podocyte progenitors toward the midline to enclose the blood vessels. However, this hypothesis needs to be addressed in a future study.

Is blood flow involved in glomerular capillary formation during mammalian metanephric development? In mammals, glomerular capillary formation is thought to begin with single capillary loop invasion into the glomerular cleft. However, a recent mouse study showed that capillaries first form a vascular network surrounding the renal vesicle before their invasion of the cleft (44). This vascular network is reminiscent of the capillaries surrounding glomerular primordia in the developing zebrafish pronephros. Our data showed such capillaries subsequently to be incorporated into and remodeled in the glomerular primordia in a flow-dependent manner. Hence, blood flow might regulate glomerular capillary formation during the process of metanephric development. This hypothesis is supported by a report showing that kidney organoids exhibited enhanced glomerular vascularization when cultured *in vitro* under high fluid flow conditions during nephrogenesis while remaining largely avascular under static conditions (45). Thus, elucidation of the blood-flow requirement for glomerular capillary development in the mammalian metanephros, and its underlying mechanisms, awaits future study.

Disclosures

All authors have nothing to disclose.

Funding

This work was supported by the Japan Agency for Medical Research and Development (AMED) (grant JP17gm5810010) to S. Fukuhara; by Grants-in-Aid for Scientific Research (B) (grant 16H05125) to S. Fukuhara; by the Japan Society for the Promotion of Science (grants 17K19689, 19K22517) for exploratory research to S. Fukuhara; and research grants from Takeda Science Foundation, the Naito Foundation, Daiichi Sankyo Foundation of Life Science, Astellas Foundation for Research on Metabolic Disorders, the Princess Takamatsu Cancer Research Fund, the NOVARTIS Foundation (Japan) for the Promotion of Science, the Uehara Memorial Foundation, and the Terumo Life Science Foundation to S. Fukuhara.

Acknowledgments

We thank Christoph Englert (Leibniz Institute on Aging–Fritz Lipmann Institute) for *Tg(wt1a:eGFP)*, D.Y. Stainier (Max Planck Institute for Heart and Lung Research) for *Tg(kdrl:tagBFP)*^{mu293Tg}, K. Kawakami (National Institute of Genetics) for *Tg(UAS:eGFP)* and the Tol2 system, and S. Schulte-Merker (University of Münster, Germany) for the Tol2_amp and pCS2_Gal4FF_KanR vectors. We also thank H. Ichimiya, E. Oguri-Nakamura, S. Egawa, and K. Kato for excellent technical assistance.

Author Contributions

K. Ando, N. Mochizuki, H. Nakajima, S. Yuge, and W. Zhou generated transgenic zebrafish; S. Fukuhara, T. Ishii, and Y. Nishimura conceived and designed the studies; S. Fukuhara and T. Ishii wrote the manuscript; T. Ishii and Y. Nishimura performed the main experiments and analyzed the data; and all authors approved the final version of the manuscript.

Supplemental Material

This article contains the following supplemental material online at http://kidney360.asnjournals.org/lookup/suppl/doi:10.34067/KID.0005962021/-/DCSupplemental.

Supplemental Figure 1. Differentiation of podocytes during pronephric glomerulus development.

Supplemental Figure 2. Differentiation of mesangial cells during pronephric glomerulus development.

Supplemental Figure 3. *vegfaa* promoter-driven expression of destabilized enhanced green fluorescent protein in the somites of zebrafish embryos.

Supplemental Movie 1. Dorsal to ventral confocal z-stack series of the pronephric glomerulus in *Tg(wt1a:eGFP);Tg(fli1a:MyrmCherry)* embryos at 28 hours post fertilization (hpf) as observed in Figure 1B.

Supplemental Movie 2. Dorsal to ventral confocal z-stack series of the pronephric glomerulus in *Tg(wt1a:eGFP);Tg(fli1a:MyrmCherry)* embryos at 32 hpf as observed in Figure 1B.

Supplemental Movie 3. Dorsal to ventral confocal z-stack series of the pronephric glomerulus in *Tg(wt1a:eGFP);Tg(fli1a:MyrmCherry)* embryos at 39 hpf as observed in Figure 1B.

Supplemental Movie 4. Dorsal to ventral confocal z-stack series of the pronephric glomerulus in *Tg(wt1a:eGFP);Tg(fli1a:MyrmCherry)* embryos at 48 hpf as observed in Figure 1B.

Supplemental Movie 5. Dorsal to ventral confocal z-stack series of the pronephric glomerulus in *Tg(wt1a:eGFP);Tg(fli1a:MyrmCherry)* embryos at 96 hpf as observed in Figure 1B.

Supplemental Movie 6. Dorsal to ventral confocal z-stack series of the pronephric glomerulus in *Tg(wt1a:eGFP);Tg(fli1a:MyrmCherry)* embryos injected with Qdot705 at 35 hpf as observed in Figure 3B.

Supplemental Movie 7. Dorsal to ventral confocal z-stack series of the pronephric glomerulus in *Tg(wt1a:eGFP);Tg(fli1a:MyrmCherry)* embryos injected with Qdot705 at 38 hpf as observed in Figure 3B.

Supplemental Movie 8. Dorsal to ventral confocal z-stack series of the pronephric glomerulus in *Tg(wt1a:eGFP);Tg(fli1a:MyrmCherry)* embryos injected with Qdot705 at 42 hpf as observed in Figure 3B.

Supplemental Movie 9. Dorsal to ventral confocal z-stack series of the pronephric glomerulus in *Tg(wt1a:eGFP);Tg(fli1a:Myr-mCherry)* embryos injected with Qdot705 at 46 hpf as observed in Figure 3B.

Supplemental Movie 10. Dorsal to ventral confocal z-stack series of the pronephric glomerulus in *Tg(wt1a:eGFP);Tg(fli1a:Myr-mCherry)* embryos injected with Qdot705 at 48 hpf as observed in Figure 3B.

Supplemental Movie 11. Dorsal to ventral confocal z-stack series of the pronephric glomerulus in 54 hpf *Tg(wt1a:eGFP);Tg(fli1a:Myr-mCherry)* embryos treated with vehicle from 36 hpf as observed in Figure 4D.

Supplemental Movie 12. Dorsal to ventral confocal z-stack series of the pronephric glomerulus in 54 hpf *Tg(wt1a:eGFP);Tg(fli1a:Myr-mCherry)* embryos treated with 2,3-butanedione monoxime (BDM) from 36 hpf as observed in Figure 4D.

Supplemental Movie 13. Dorsal to ventral confocal z-stack series of the pronephric glomerulus in 54 hpf *Tg(wt1a:eGFP);Tg(fli1a:Myr-mCherry)* embryos treated with tricine from 36 hpf as observed in Figure 4D.

Supplemental Movie 14. Time-lapse confocal imaging of morphogenetic processes of pronephric glomeruli in *Tg(wt1a:eGFP); Tg(fli1a:Myr-mCherry)* embryos as observed in Figure 5A.

Supplemental Movie 15. Time-lapse confocal imaging of morphogenetic processes of pronephric glomeruli in *Tg(wt1a:eGFP); Tg(fli1a:Myr-mCherry)* embryos in the presence of BDM as observed in Figure 5B.

References

1. Pollak MR, Quaggin SE, Hoenig MP, Dworkin LD: The glomerulus: The sphere of influence. *Clin J Am Soc Nephrol* 9: 1461–1469, 2014 https://doi.org/10.2215/CJN.09400913
2. Scott RP, Quaggin SE: Review series: The cell biology of renal filtration. *J Cell Biol* 209: 199–210, 2015 https://doi.org/10.1083/jcb.201410017
3. Vaughan MR, Quaggin SE: How do mesangial and endothelial cells form the glomerular tuft? *J Am Soc Nephrol* 19: 24–33, 2008 https://doi.org/10.1681/ASN.2007040471
4. Schell C, Wanner N, Huber TB: Glomerular development—Shaping the multi-cellular filtration unit. *Semin Cell Dev Biol* 36: 39–49, 2014 https://doi.org/10.1016/j.semcdb.2014.07.016
5. Robert B, Zhao X, Abrahamson DR: Coexpression of neuropilin-1, Flk1, and VEGF(164) in developing and mature mouse kidney glomeruli. *Am J Physiol Renal Physiol* 279: F275–F282, 2000 https://doi.org/10.1152/ajprenal.2000.279.2.F275
6. Eremina V, Sood M, Haigh J, Nagy A, Lajoie G, Ferrara N, Gerber HP, Kikkawa Y, Miner JH, Quaggin SE: Glomerular-specific alterations of VEGF-A expression lead to distinct congenital and acquired renal diseases. *J Clin Invest* 111: 707–716, 2003 https://doi.org/10.1172/JCI17423
7. Potter EL: Development of the human glomerulus. *Arch Pathol* 80: 241–255, 1965
8. Taguchi A, Kaku Y, Ohmori T, Sharmin S, Ogawa M, Sasaki H, Nishinakamura R: Redefining the *in vivo* origin of metanephric nephron progenitors enables generation of complex kidney structures from pluripotent stem cells. *Cell Stem Cell* 14: 53–67, 2014 https://doi.org/10.1016/j.stem.2013.11.010
9. Takasato M, Er PX, Chiu HS, Maier B, Baillie GJ, Ferguson C, Parton RG, Wolvetang EJ, Roost MS, Chuva de Sousa Lopes SM, Little MH: Kidney organoids from human iPS cells contain multiple lineages and model human nephrogenesis [published correction appears in *Nature* 536: 238, 2016 https://doi.org/10.1038/nature17982]. *Nature* 526: 564–568, 2015 https://doi.org/10.1038/nature17982
10. Morizane R, Lam AQ, Freedman BS, Kishi S, Valerius MT, Bonventre JV: Nephron organoids derived from human pluripotent stem cells model kidney development and injury. *Nat Biotechnol* 33: 1193–1200, 2015 https://doi.org/10.1038/nbt.3392
11. Sharmin S, Taguchi A, Kaku Y, Yoshimura Y, Ohmori T, Sakuma T, Mukoyama M, Yamamoto T, Kurihara H, Nishinakamura R: Human induced pluripotent stem cell–derived podocytes mature into vascularized glomeruli upon experimental transplantation. *J Am Soc Nephrol* 27: 1778–1791, 2016 https://doi.org/10.1681/ASN.2015010096
12. Bantounas I, Ranjzad P, Tengku F, Silajdžić E, Forster D, Asselin MC, Lewis P, Lennon R, Plagge A, Wang Q, Woolf AS, Kimber SJ: Generation of functioning nephrons by implanting human pluripotent stem cell–derived kidney progenitors. *Stem Cell Reports* 10: 766–779, 2018 https://doi.org/10.1016/j.stemcr.2018.01.008
13. Drummond I: Making a zebrafish kidney: A tale of two tubes. *Trends Cell Biol* 13: 357–365, 2003 https://doi.org/10.1016/S0962-8924(03)00124-7
14. Drummond IA: Kidney development and disease in the zebrafish. *J Am Soc Nephrol* 16: 299–304, 2005 https://doi.org/10.1681/ASN.2004090754
15. Kroeger PT Jr, Drummond BE, Miceli R, McKernan M, Gerlach GF, Marra AN, Fox A, McCampbell KK, Leshchiner I, Rodriguez-Mari A, BreMiller R, Thummel R, Davidson AJ, Postlethwait J, Goessling W, Wingert RA: The zebrafish kidney mutant *zeppelin* reveals that *brca2/fancd1* is essential for pronephros development. *Dev Biol* 428: 148–163, 2017 https://doi.org/10.1016/j.ydbio.2017.05.025
16. Poureetezadi SJ, Wingert RA: Little fish, big catch: Zebrafish as a model for kidney disease. *Kidney Int* 89: 1204–1210, 2016 https://doi.org/10.1016/j.kint.2016.01.031
17. Ichimura K, Bubenshchikova E, Powell R, Fukuyo Y, Nakamura T, Tran U, Oda S, Tanaka M, Wessely O, Kurihara H, Sakai T, Obara T: A comparative analysis of glomerulus development in the pronephros of medaka and zebrafish. *PLoS One* 7: e45286, 2012 https://doi.org/10.1371/journal.pone.0045286
18. Drummond IA, Majumdar A, Hentschel H, Elger M, Solnica-Krezel L, Schier AF, Neuhauss SC, Stemple DL, Zwartkruis F, Rangini Z, Driever W, Fishman MC: Early development of the zebrafish pronephros and analysis of mutations affecting pronephric function. *Development* 125: 4655–4667, 1998 https://doi.org/10.1242/dev.125.23.4655
19. Zhou W, Boucher RC, Bollig F, Englert C, Hildebrandt F: Characterization of mesonephric development and regeneration using transgenic zebrafish. *Am J Physiol Renal Physiol* 299: F1040–F1047, 2010 https://doi.org/10.1152/ajprenal.00394.2010
20. Diep CQ, Peng Z, Ukah TK, Kelly PM, Daigle RV, Davidson AJ: Development of the zebrafish mesonephros. *Genesis* 53: 257–269, 2015 https://doi.org/10.1002/dvg.22846
21. Wingert RA, Selleck R, Yu J, Song HD, Chen Z, Song A, Zhou Y, Thisse B, Thisse C, McMahon AP, Davidson AJ: The cdx genes and retinoic acid control the positioning and segmentation of the zebrafish pronephros. *PLoS Genet* 3: e189, 2007 https://doi.org/10.1371/journal.pgen.0030189
22. Fukuhara S, Zhang J, Yuge S, Ando K, Wakayama Y, Sakaue-Sawano A, Miyawaki A, Mochizuki N: Visualizing the cell-cycle progression of endothelial cells in zebrafish. *Dev Biol* 393: 10–23, 2014 https://doi.org/10.1016/j.ydbio.2014.06.015
23. Kimmel CB, Ballard WW, Kimmel SR, Ullmann B, Schilling TF: Stages of embryonic development of the zebrafish. *Dev Dyn* 203: 253–310, 1995 https://doi.org/10.1002/aja.1002030302
24. Kawakami K, Takeda H, Kawakami N, Kobayashi M, Matsuda N, Mishina M: A transposon-mediated gene trap approach identifies developmentally regulated genes in zebrafish. *Dev Cell* 7: 133–144, 2004 https://doi.org/10.1016/j.devcel.2004.06.005
25. Bussmann J, Schulte-Merker S: Rapid BAC selection for tol2-mediated transgenesis in zebrafish. *Development* 138: 4327–4332, 2011 https://doi.org/10.1242/dev.068080
26. Ando K, Fukuhara S, Izumi N, Nakajima H, Fukui H, Kelsh RN, Mochizuki N: Clarification of mural cell coverage of vascular endothelial cells by live imaging of zebrafish. *Development* 143: 1328–1339, 2016 https://doi.org/10.1242/dev.132654
27. Bollig F, Perner B, Besenbeck B, Köthe S, Ebert C, Taudien S, Englert C: A highly conserved retinoic acid responsive element controls wt1a expression in the zebrafish pronephros.

Development 136: 2883–2892, 2009 https://doi.org/10.1242/dev.031773
28. Asakawa K, Suster ML, Mizusawa K, Nagayoshi S, Kotani T, Urasaki A, Kishimoto Y, Hibi M, Kawakami K: Genetic dissection of neural circuits by Tol2 transposon-mediated Gal4 gene and enhancer trapping in zebrafish. *Proc Natl Acad Sci U S A* 105: 1255–1260, 2008 https://doi.org/10.1073/pnas.0704963105
29. Zhou W, Hildebrandt F: Inducible podocyte injury and proteinuria in transgenic zebrafish. *J Am Soc Nephrol* 23: 1039–1047, 2012 https://doi.org/10.1681/ASN.2011080776
30. Liang D, Chang JR, Chin AJ, Smith A, Kelly C, Weinberg ES, Ge R: The role of vascular endothelial growth factor (VEGF) in vasculogenesis, angiogenesis, and hematopoiesis in zebrafish development. *Mech Dev* 108: 29–43, 2001 https://doi.org/10.1016/S0925-4773(01)00468-3
31. Majumdar A, Drummond IA: The zebrafish floating head mutant demonstrates podocytes play an important role in directing glomerular differentiation. *Dev Biol* 222: 147–157, 2000 https://doi.org/10.1006/dbio.2000.9642
32. Kubo K, Shimizu T, Ohyama S, Murooka H, Iwai A, Nakamura K, Hasegawa K, Kobayashi Y, Takahashi N, Takahashi K, Kato S, Izawa T, Isoe T: Novel potent orally active selective VEGFR-2 tyrosine kinase inhibitors: Synthesis, structure-activity relationships, and antitumor activities of *N*-phenyl-*N*′-4-(4-quinolyloxy)phenylureas. *J Med Chem* 48: 1359–1366, 2005 https://doi.org/10.1021/jm030427r
33. Ostap EM: 2,3-Butanedione monoxime (BDM) as a myosin inhibitor. *J Muscle Res Cell Motil* 23: 305–308, 2002 https://doi.org/10.1023/A:1022047102064
34. Carter KM, Woodley CM, Brown RS: A review of tricaine methanesulfonate for anesthesia of fish. *Rev Fish Biol Fish* 21: 51–59, 2011 https://doi.org/10.1007/s11160-010-9188-0
35. Attili S, Hughes SM: Anaesthetic tricaine acts preferentially on neural voltage-gated sodium channels and fails to block directly evoked muscle contraction. *PLoS One* 9: e103751, 2014 https://doi.org/10.1371/journal.pone.0103751
36. Serluca FC, Drummond IA, Fishman MC: Endothelial signaling in kidney morphogenesis: A role for hemodynamic forces. *Curr Biol* 12: 492–497, 2002 https://doi.org/10.1016/S0960-9822(02)00694-2
37. Brown S, Bernardo MM, Li Z-H, Kotra LP, Tanaka Y, Fridman R, Mobashery S: Potent and selective mechanism-based inhibition of gelatinases. *J Am Chem Soc* 122: 6799–6800, 2000 https://doi.org/10.1021/ja001461n
38. Hahn C, Schwartz MA: Mechanotransduction in vascular physiology and atherogenesis. *Nat Rev Mol Cell Biol* 10: 53–62, 2009 https://doi.org/10.1038/nrm2596
39. Ando J, Yamamoto K: Flow detection and calcium signalling in vascular endothelial cells. *Cardiovasc Res* 99: 260–268, 2013 https://doi.org/10.1093/cvr/cvt084
40. Nakajima H, Yamamoto K, Agarwala S, Terai K, Fukui H, Fukuhara S, Ando K, Miyazaki T, Yokota Y, Schmelzer E, Belting HG, Affolter M, Lecaudey V, Mochizuki N: Flow-dependent endothelial YAP regulation contributes to vessel maintenance. *Dev Cell* 40: 523–536.e6, 2017 https://doi.org/10.1016/j.devcel.2017.02.019
41. Chen Q, Jiang L, Li C, Hu D, Bu JW, Cai D, Du JL: Haemodynamics-driven developmental pruning of brain vasculature in zebrafish. *PLoS Biol* 10: e1001374, 2012 https://doi.org/10.1371/journal.pbio.1001374
42. Meeson A, Palmer M, Calfon M, Lang R: A relationship between apoptosis and flow during programmed capillary regression is revealed by vital analysis. *Development* 122: 3929–3938, 1996 https://doi.org/10.1242/dev.122.12.3929
43. Wang Y, Kaiser MS, Larson JD, Nasevicius A, Clark KJ, Wadman SA, Roberg-Perez SE, Ekker SC, Hackett PB, McGrail M, Essner JJ: Moesin1 and Ve-cadherin are required in endothelial cells during *in vivo* tubulogenesis. *Development* 137: 3119–3128, 2010 https://doi.org/10.1242/dev.048785
44. Yu T, Zhang F, Wu Y, Chen J, Dai L, Li F, Liu X, Liu C, Zhao J: Detailed process analysis for glomerular capillary formation by immunofluorescence on ultra-thick sections [published correction appears in *Gene Expr Patterns* 38: 119143 https://doi.org/10.1016/j.gep.2020.119143]. *Gene Expr Patterns* 35: 119096, 2020 https://doi.org/10.1016/j.gep.2020.119096
45. Homan KA, Gupta N, Kroll KT, Kolesky DB, Skylar-Scott M, Miyoshi T, Mau D, Valerius MT, Ferrante T, Bonventre JV, Lewis JA, Morizane R: Flow-enhanced vascularization and maturation of kidney organoids *in vitro*. *Nat Methods* 16: 255–262, 2019 https://doi.org/10.1038/s41592-019-0325-y

Received: September 10, 2021 **Accepted:** January 18, 2022

Y.N. and T.I. contributed equally to this work.